

## Structure-based design and subsequent optimization of 2-tolyl-(1,2,3-triazol-1-yl-4-carboxamide) inhibitors of p38 MAP kinase

D. A. Cogan,<sup>a,\*</sup> R. Aungst,<sup>d</sup> E. C. Breinlinger,<sup>d,†</sup> T. Fadra,<sup>a</sup> D. R. Goldberg,<sup>a</sup> M. H. Hao,<sup>a</sup> R. Kroe,<sup>c</sup> N. Moss,<sup>a</sup> C. Pargellis,<sup>b</sup> K. C. Qian<sup>a</sup> and A. D. Swinamer<sup>a</sup>

<sup>a</sup>Department of Medicinal Chemistry, Boehringer Ingelheim Pharmaceuticals, Inc., Research and Development Center, 900 Ridgebury Road, PO Box 368, Ridgefield, CT 06877, USA

<sup>b</sup>Department of Immunology and Inflammation, Boehringer Ingelheim Pharmaceuticals, Inc., Research and Development Center, 900 Ridgebury Road, Ridgefield, CT 06877, USA

<sup>c</sup>Department of Biologics and Biomolecular Sciences, Boehringer Ingelheim Pharmaceuticals, Inc., Research and Development Center, 900 Ridgebury Road, Ridgefield, CT 06877, USA

<sup>d</sup>Medicinal Chemistry, AMRI, 30 Corporate Circle, Albany, NY 12203, USA

Received 22 February 2008; revised 15 April 2008; accepted 21 April 2008

Available online 25 April 2008

**Abstract**—A computer-aided drug design strategy leads to the identification of a new class of p38 inhibitors based on the 2-tolyl-(1,2,3-triazol-1-yl-4-carboxamide) scaffold. The tolyl triazole amides provided a potent platform amenable to optimization. Further exploration leads to compounds with greater than 100-fold improvement in binding affinity to p38. Derivatives prepared to alter the physicochemical properties produced inhibitors with IC<sub>50</sub>'s in human whole blood as low as 83 nM.  
© 2008 Elsevier Ltd. All rights reserved.

The mitogen-activated protein (MAP) kinase p38 is a key regulator in the signaling pathways controlling the production of pro-inflammatory cytokines such as TNF- $\alpha$  and IL-1 $\beta$ .<sup>1</sup> Therefore, the identification of p38 inhibitors has been the focus of intense research.<sup>2</sup> This effort has been bolstered by the recent clinical and commercial success of anti-cytokine biologics such as Enbrel<sup>®</sup>, Remicade<sup>®</sup>, Humira<sup>®</sup>, and Kineret<sup>®</sup> for the treatment of various autoimmune diseases.<sup>3</sup> It is anticipated that small molecule inhibitors of p38 will provide at least a similar therapeutic benefit as anti-cytokine biologics, but with the convenience of oral dosage.

We have previously described naphthyl urea-based inhibitors, such as the clinical compound **BIRB 796**, that bind to what we call the 'Phe-out' conformation of p38.<sup>4</sup> In addition to the conventional H-bonding interaction

with Met109 in the ATP binding site and hydrophobic contacts in the adjacent kinase specificity pocket, this class of compounds takes advantage of additional binding sites made available by the movement of Phe169. Thus, the *tert*-butyl pyrazole replaces Phe169 in the 'Phe pocket' while the urea takes part in a hydrogen bonding network with the backbone NH of Asp168

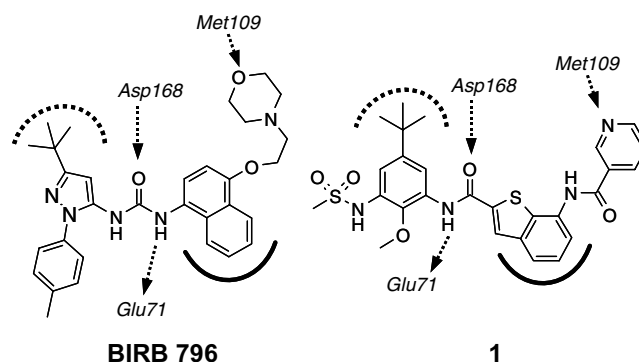


**Figure 1.** Representative inhibitors highlighting key interactions with p38. The dotted arc represents the Phe-pocket, and the solid arc represents the kinase specificity pocket.

**Keywords:** p38 kinase; p38a; p38; p38 MAPK; MAP kinase; Inhibitors; Triazoles; Structure-based drug design.

\* Corresponding author. Tel.: +1 203 791 6187; fax: +1 203 791 6072; e-mail: [derek.cogan@boehringer-ingelheim.com](mailto:derek.cogan@boehringer-ingelheim.com)

† Present address: Abbott Bioresearch Center, 381 Plantation St., Worcester, MA 01605, USA.

and the carboxylate of Glu71 (Fig. 1).<sup>5</sup> By taking advantage of these interactions, the naphthyl urea class of inhibitors can achieve  $K_D$ 's below 1 nM.

The success of **BIRB 796** established inhibition of the Phe-out conformation as a viable path to the clinic. We were, therefore, interested in further capitalizing on the potency achievable with Phe-out binders, but also wished to explore structurally distinct scaffolds. To this end, we employed a computer aided design strategy that successfully conceived a new class of p38 inhibitors, exemplified by **1** (Fig. 1).<sup>6</sup> Herein, we describe how we have designed and optimized another novel and potent series of Phe-out p38 inhibitors based on the 2-tolyl-(1,2,3-triazol-1-yl-4-carboxamide) scaffold.

Our strategy used LigBuilder<sup>6b</sup> software to link two seed structures set in a model of the p38 active site (Fig. 2). We chose a *tert*-butyl phenyl fragment known to bind in the Phe pocket as one seed.<sup>7</sup> To this fragment we appended an *N*-formyl group to access the hydrogen bonds with Glu71 and Asp168 commonly associated with inhibitors that bind in the Phe-out conformation. Whereas a pyridyl fragment was chosen as the second seed in the design of **1**, we chose a carbonyl fragment to access the hydrogen bond with Met109. The software then used a stochastic approach to attach fragments that would link the formyl group to the carbonyl, filling the kinase specificity pocket along the way.

A 4-tolyl group situated in the kinase specificity pocket emerged from the LigandBuilder dataset as a recurring and exploitable motif. However, the dataset provided a variety of impractical flexible groups to connect the tolyl group to the carbonyl. We modeled options to constrain these flexible linkages, and predicted that *N*-linked azoles would be suitable. The five-membered ring would provide the necessary rigidity and display the carbonyl at the proper distance to interact with Met109. Modeling also indicated that connecting to the tolyl group via an *N*-linkage, as opposed to a *C*-linkage, would favor the desired out-of-plane conformation. This conformation would also be reinforced by the methyl of the tolyl core (Fig. 3). We determined previously that the presence of the methanesulfonamide of the left-hand phenyl imparted both an improvement in potency and solubility,<sup>7</sup> and thus added this group to our test series.

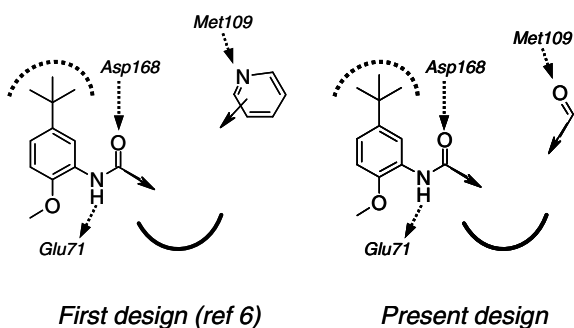


**Figure 2.** Schematics of the de novo design processes. The dotted arcs represent the Phe-pocket, and the solid arcs represent the kinase specificity pocket.

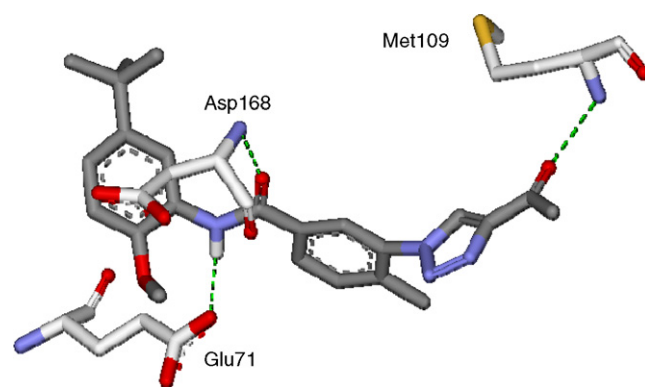
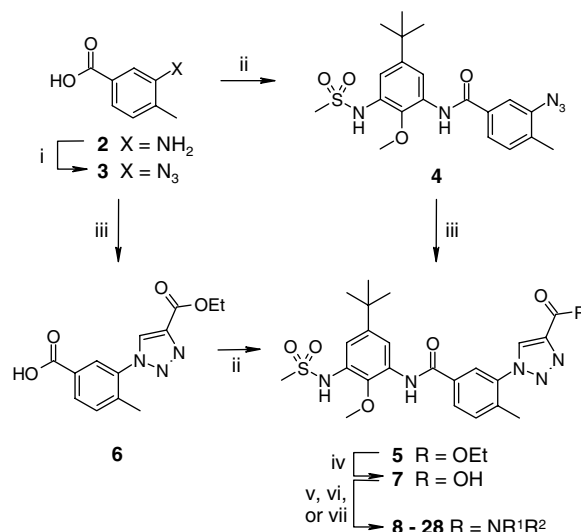


**Figure 3.** Predicted binding conformation of the designed inhibitor class highlighting key interactions with p38.

We chose 1,2,3-triazole-4-carboxamides as our specific inhibitor class due to their synthetic accessibility. This allowed us to quickly test the potency of our design, and additionally provided a synthetic handle for further SAR exploration. The synthesis of these inhibitors is outlined in Scheme 1. Diazotization of 2-amino-3-methyl benzoic acid (**2**) and subsequent displacement with sodium azide provided **3**. Amide formation with *N*-(3-amino-5-*tert*-butyl-2-methoxy-phenyl)-methanesulfonamide<sup>6</sup> provided 3-azido-amide **4**. Huisgen triazole formation with ethyl propiolate provided the triazole ester **5**. Ester **5** could also be prepared by submitting the azide **3** to the Huisgen conditions to provide ester **6**, followed by amide formation with *N*-(3-amino-5-*tert*-butyl-2-methoxy-phenyl)-methane-sulfonamide. Saponification of **5** provided triazole carboxylic acid **7**. Standard amide coupling procedures provided amides **8–28**.

Binding affinity to p38 was determined by a thermal denaturation assay.<sup>8</sup> Compounds were additionally



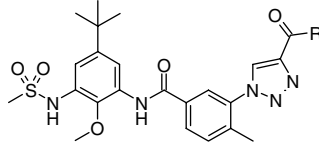
**Scheme 1.** Reagents and conditions: (i)  $\text{NaNO}_2$ , 2 M HCl,  $\text{NaN}_3$  (88%). (ii) a— $(\text{COCl})_2$ , cat. DMF; b—*N*-(3-amino-5-*tert*-butyl-2-methoxy-phenyl)-methanesulfonamide,  $\text{Et}_3\text{N}$  or 2,6-lutidine (95–98%). (iii) Ethyl propiolate, DMA, 90 °C (**5**: 62%; **6**: 48%). (iv) NaOH, MeOH (95%). (v) EDC, HOBT,  $\text{HNR}^1\text{R}^2$  (44–62%) (vi) HATU, HOAT,  $i\text{Pr}_2\text{NEt}$ ,  $\text{HNR}^1\text{R}^2$  (50–51%) (vii) a— $(\text{COCl})_2$ , cat. DMF. b— $\text{HNR}^1\text{R}^2$ ,  $\text{Et}_3\text{N}$  or 2,6-lutidine (77%).

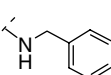
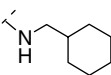
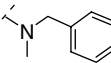
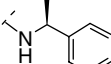
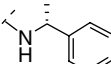
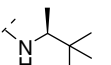
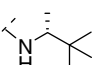
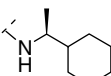
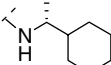
screened for inhibition of TNF- $\alpha$  production from LPS-stimulated THP-1 cells and human whole blood.<sup>4</sup> We were delighted to discover that the prototypical compound, ester **5** (Table 1), demonstrated that the design can produce potent inhibitors of p38 (a  $T_m$  of 56.2 °C corresponds to a  $K_D$  of approximately 8 nM).<sup>8</sup> The amides **8–14** demonstrated that a variety of substitutions are tolerated, and that specific substitution can lead to an increase in molecular potency.<sup>8</sup> Compounds **11** and **12** are noteworthy as

examples with greater potency in whole blood than **BIRB 796**.

We obtained a crystal structure of compound **11** bound to p38.<sup>9</sup> As expected, compound **11** bound to the Phe-out conformation with the Phe-out seed accessing the requisite hydrophobic and hydrogen-bonding interactions. In addition, the tolyl group fits tightly into the kinase specificity pocket and the right-side amide carbonyl engages Met109 in a hydrogen bond as we had pre-

**Table 1.** Molecular and cellular potencies of tolyl triazole p38 inhibitors



Compounds	R	$T_m^a$ (°C)	THP-1 $IC_{50}^b$ (nM)	Human whole blood $IC_{50}^c$ (nM)
<b>BIRB 796</b>		63.5	18 ± 2.1	780
<b>5</b>	OEt	56.2	>5000	9000 ± 1700
<b>8</b>		57.3	110 ( $n = 1$ )	8400 ± 1500
<b>9</b>		56.6	110 ( $n = 1$ )	2800 ± 830
<b>10</b>		56.8	84 ( $n = 1$ )	>15,000
<b>11</b>		59.7	40 ± 35	930 ± 220
<b>12</b>		60.5	14 ± 4.2	260 ± 120
<b>13</b>		56.2	14 ± 1.5	260 ± 84
<b>14</b>		57.8	29 ( $n = 1$ )	>15,000
<b>15</b>		60.1	27 ± 6.7	2600 ± 1300
<b>16</b>		64.6	13 ± 1.2	470 ± 170
<b>17</b>		60.0	35 ( $n = 1$ )	2600 ± 1,000
<b>18</b>		61.6 ± 0.1	14 ± 1.4	1,000 ± 630
<b>19</b>		56.9	66 ( $n = 1$ )	5600 ± 2700
<b>20</b>		60.8 ± 0.0	16 ± 0.71	2800 ± 2500

<sup>a</sup> Thermal denaturation. See Ref. 7. Data are from a single experiment unless a standard deviation is provided.

<sup>b</sup> Inhibition of TNF $\alpha$  production in LPS-challenged THP-1 cells.

<sup>c</sup> Inhibition of TNF $\alpha$  production in LPS-challenged human whole blood; average of at least three values from at least three individual donors.

dicted. Moreover, the overall conformation of the crystal structure is similar to the modeled conformation. Interestingly, the benzyl group also formed an induced-fit interaction with a hydrophobic pocket formed

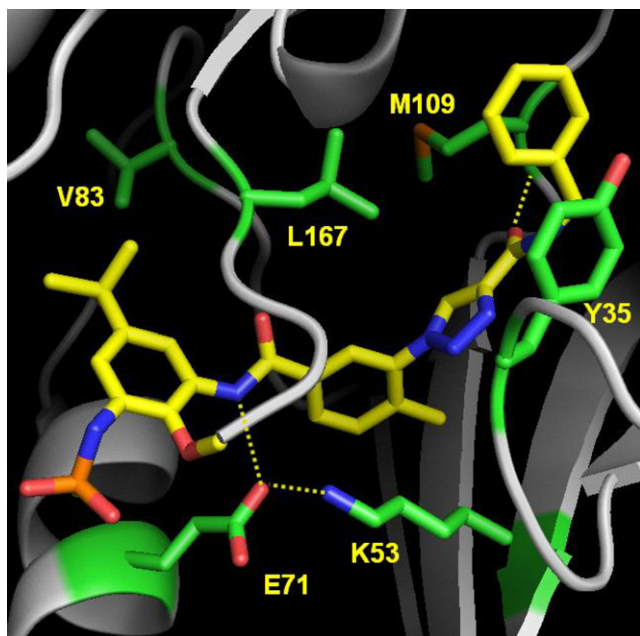


Figure 4. Crystal structure of **11** bound to p38.

from the side-chains of Tyr35, Leu167, and Met109 (Fig. 4), providing a rationale for the increase in potency observed for some of the larger lipophilic amides. Similar interactions have been reported for ATP-site only inhibitors of p38.<sup>10</sup> The NH of the benzyl amide does not play a direct role in binding to p38, consistent with the modest loss on binding potency observed for **14** when compared to **11**.

The crystal structure of **11** suggested that substitution at the  $\alpha$ -position of the benzyl group should be tolerated and might provide a beneficial conformational constraint. Compounds **15–20** highlight the effect of  $\alpha$ -methyl substitution (Table 1). The R-enantiomer consistently demonstrated an increase in  $T_m$ , although this benefit did not consistently translate to improved potency in cellular assays (e.g. **15** vs. **16**).

By exploring the amide region of the inhibitors, we had discovered a number of potent compounds with reasonable potencies in cell assays. However, these compounds suffered from poor aqueous solubility (typically  $<1 \mu\text{g}/\text{mL}$ ). Although the crystal structure of **11** indicated that the amide substituents occupy a largely lipophilic region, due to the proximity of the solvent interface we felt that polar substitution may also be tolerated in this region. Therefore, an additional set of amides with polar functionality were prepared and were also found to be potent p38 inhibitors (Table 2). One interesting example

Table 2. Molecular and cellular potencies for tolyl triazole p38 inhibitors

Compounds	R	$T_m^a$ (°C)	THP-1 $\text{IC}_{50}^b$ (nM)	Human whole blood $\text{IC}_{50}^c$ (nM)
<b>21</b>		57.9	$38 \pm 11$	$270 \pm 110$
<b>22</b>		58.8	$74 \pm 14$	$720 \pm 220$
<b>23</b>		65.1	$35 (n = 1)$	$500 \pm 220$
<b>24</b>		59.9	$18 (n = 1)$	$210 \pm 90$
<b>25</b>		56.1	$140 (n = 1)$	$790 \pm 680$
<b>26</b> <sup>11</sup>		57.4	$28 (n = 1)$	$300 \pm 180$
<b>27</b> <sup>11</sup>		57.5	$200 (n = 1)$	$4500 \pm 2100$
<b>28</b>		$57.3 \pm 1.9$	$22 \pm 2.1$	$83 \pm 52$

<sup>a,b,c</sup>See footnotes for Table 1.

**Table 3.** Relationship between physicochemical properties and potency in human whole blood for select compounds

Compound	$T_m$ (°C)	Human whole blood $IC_{50}$ (nM)	Solubility in pH 7.4 buffer ( $\mu\text{g/mL}$ )	Caco-2 $P_{app} \times 10^{-6}$ (cm/s)	Plasma protein binding (%)
<b>BIRB796</b>	63.5	780	1.0	10	99
<b>12</b>	60.5	260	bq <sup>a</sup>	<sup>b</sup>	92
<b>24</b>	59.9	210	2.0	7.4	66
<b>28</b>	57.3	83	13.9	13	66

<sup>a</sup> Below quantifiable limit: 0.1  $\mu\text{g/mL}$ .

<sup>b</sup> Insufficient solubility for assay.

is compound **28**, whose  $IC_{50}$  in whole blood is 83 nM despite having a  $T_m$  3 °C lower than **12**.

Efficacy in the human whole blood assay can be attributed to a variety of factors, including plasma protein binding (affinity and kinetics), and membrane permeability, that should be dependant upon a compound's physicochemical properties. Table 3 indicates how solubility, permeability, and plasma protein binding relate to whole blood potency for select compounds. While it appears that permeability is not a determining factor for these compounds, the extent of protein binding does have an impact. As a result, compound **28** is almost 10-fold more potent in whole blood than **BIRB 796** despite having a  $T_m$  more than 6 °C lower.

It is worth noting that the compounds from this series typically demonstrate a high level of kinase selectivity, even among kinases that the naphthyl ureas typically inhibit. For example, whereas **BIRB 796** has an  $IC_{50}$  for Jnk2a of 6 nM, the  $IC_{50}$  for compound **28** is 1.1  $\mu\text{M}$ . In addition, **28** does not demonstrate activity against the following kinases at 3  $\mu\text{M}$ : MKK1, ERK2, JNK1, p38 $\gamma$ , p38 $\delta$ , MAPKAP-K1a, MAPKAP-K2, MSK1, PRAK, PKA, PKC $\alpha$ , PDK1, PKB $\delta$ PH, SGK, S6K1, GSK3 $\beta$ , ROCK-II, AMPK, CHK1, CK2, PHOS. KINASE, CDK2/cyclin A, CK1, DYRK1A, PP2A, and NEK6, and the following tested at 10  $\mu\text{M}$ : Btk, Eck, EGFR, FGFR3, Hek, HGFR, IGF1R, IR, Itk, JAK3, Lyn, Syk, TXK, VEGFR1.

Our de novo design strategy has provided access to an additional structurally distinct class of p38 inhibitors. This work highlights an example of using computer-aided drug design to generate ideas, and molecular modeling to refine these ideas into viable lead structures. The design provided potent p38 inhibitors that were amenable to analogue synthesis, allowing the further improvement in physicochemical properties and potency in human whole blood.

## References and notes

- (a) Wagner, G.; Laufer, S. *Med. Res. Rev.* **2006**, *26*, 1; (b) Saklatvala, J. *Curr. Opin. Pharm.* **2004**, *4*, 372; (c) Kumar, S.; Boehm, J.; Lee, J. C. *Nature Rev. Drug Discov.* **2003**, *2*, 717; (d) Ono, K.; Han, J. *Cell. Signal.* **2000**, *12*, 1.
- (a) Dominguez, C.; Powers, D. A.; Tamayo, N. *Curr. Opin. Drug Disc. Dev.* **2005**, *8*, 421; (b) Nikas, S. N.; Drosos, A. A. *Curr. Opin. Invest. Drugs* **2004**, *5*, 1205; (c) Cirillo, P. F.; Pargellis, C.; Regan, J. *Curr. Topics Med. Chem.* **2002**, *2*, 1021.
- (a) Klinkhoff, A. *Drugs* **2004**, *64*, 1267; (b) Barry, J.; Kirby, B. *Expert Opin. Biol. Ther.* **2004**, *4*, 975.
- (a) Regan, J.; Breitfelder, S.; Cirillo, P.; Gilmore, T.; Graham, A. G.; Hickey, E. R.; Klaus, B.; Madwed, J.; Moriak, M.; Moss, N.; Pargellis, C. A.; Pav, S.; Proto, A.; Swinamer, A.; Tong, L.; Torcellini, C. *J. Med. Chem.* **2002**, *45*, 2994; (b) Regan, J.; Capolino, A.; Cirillo, P. F.; Gilmore, T.; Graham, A. G.; Hickey, E.; Kroe, R. R.; Madwed, J.; Moriak, M.; Nelson, R.; Pargellis, C. A.; Swinamer, A.; Torcellini, C.; Tsang, M.; Moss, N. *J. Med. Chem.* **2003**, *46*, 4676.
- Pargellis, C. A.; Tong, L.; Churchill, L.; Cirillo, P.; Gilmore, T.; Graham, A. G.; Grob, P. M.; Hickey, E. R.; Moss, N.; Pav, S.; Regan, J. *Nat. Struct. Biol.* **2002**, *9*, 268.
- (a) Goldberg, D.; Hao, M.-H.; Qian, K. C.; Swinamer, A. D.; Gao, D. A.; Xiong, Z.; Sarko, C.; Berry, A.; Lord, J.; Magolda, R. L.; Fadra, T.; Kroe, R. R.; Kukulka, A.; Madwed, J. B.; Martin, L.; Pargellis, C.; Skow, D.; Song, J. J.; Tan, Z.; Torcellini, C. A.; Zimmiti, C. S.; Yee, N. K.; Moss, N. *J. Med. Chem.* **2007**, *50*, 4016; (b) Wang, R.; Gao, Y.; Lai, L. *J. Mol. Model* **2000**, *6*, 498.
- SAR at this region will be disclosed in future publications.
- A 2.8 °C change in thermal denaturation temperature corresponds to approximately a 10-fold change in binding affinity. However, it must be noted that this relationship was developed for pyrazole naphthyl urea-based inhibitors (e.g., **BIRB 796**), and if the thermodynamics of binding for this class of inhibitors is significantly different, this relationship may be an approximation. Kroe, R. R.; Regan, J.; Proto, A.; Peet, G. W.; Roy, T.; Dickert, L.; Fuschetto, N.; Pargellis, C. A.; Ingraham, R. H. *J. Med. Chem.* **2003**, *46*, 4669.
- The coordinates have been deposited in the RCSB protein databank (RCSB ID code rcsb047198 and PDB ID code 3CTQ).
- Fitzgerald, C. E.; Patel, S. B.; Becker, J. W.; Cameron, P. M.; Zaller, D.; Pikounis, V. B.; O'Keefe, S. J.; Scapin, G. *Nature: Struct. Biol.* **2003**, *10*, 764.
- Compounds **26** and **27** were prepared from their N-Boc piperidine analogues via Boc-removal (HCl/dioxane; 66% yield) and reductive amination (formaldehyde, 1% HOAc in methanol, NaCNBH<sub>3</sub>, 25% yield).